

The reaction center is the sensitive target of the mercury(II) ion in intact cells of photosynthetic bacteria

Emese Asztalos · Gábor Sipka · Mariann Kis · Massimo Trotta · Péter Maróti

The publisher's version: Photosynth Res (2012) 112:129–140; DOI 10.1007/s11120-012-9749-2

Abstract

The sensitivity of intact cells of purple photosynthetic bacterium *Rhodobacter sphaeroides* wild type to low level (~100 μM) of mercury (Hg^{2+}) contamination was evaluated by absorption and fluorescence spectroscopies of the bacteriochlorophyll–protein complexes. All assays related to the function of the reaction center (RC) protein (induction of the bacteriochlorophyll fluorescence, delayed fluorescence and light-induced oxidation and reduction of the bacteriochlorophyll dimer and energization of the photosynthetic membrane) showed prompt and later effects of the mercury ions. The damage expressed by decrease of the magnitude and changes of rates of the electron transfer kinetics followed complex (spatial and temporal) pattern according to the different Hg^{2+} sensitivities of the electron transport (donor/acceptor) sites including the reduced bound and free cytochrome c_2 and the primary reduced quinone. In contrast to the RC, the light harvesting system and the bc_1 complex demonstrated much higher resistance against the mercury pollution. The 850 and 875 nm components of the peripheral and core complexes were particularly insensitive to the mercury(II) ions. The concentration of the photoactive RCs and the connectivity of the photosynthetic units decreased upon mercury treatment. The degree of inhibition of the photosynthetic apparatus was always higher when the cells were kept in the light than in the dark indicating the importance of metabolism in active transport of the mercury ions from outside to the intracytoplasmic membrane. Any of the tests applied in this study can be used for detection of changes in photosynthetic bacteria at the early stages of the action of toxicants.

Introduction

The elevated level of mercury in the environment has become a problem of current interest on a global scale. Two-third of the mercury input comes from various natural biogeochemical emissions while one-third has anthropogenic sources (Patra and Sharma 2000). Because mercury is known for non-biodegradability, translocation in the ecosystem and heavy distortion of metabolic pathways, it may cause serious biochemical and physiological disorders (Panda and Panda 2009; Barregard et al. 2010). Due to the health hazards, the detrimental effects of mercury have been studied extensively on animals and human beings (Clifton 2007). The photosynthetic organisms have received much less attention, although their significance of potential application in bioremediation cannot be overestimated (Malik 2004; Patra et al. 2004; Cain et al. 2008; Borsetti et al. 2009; Deng and Jia 2011). Extensive work has been carried out to describe and to understand the mercuric toxicity to photosynthesis of plants and algae (Kamp-Nielsen 1971; Gotsis-Skretas 1991; Boucher and Carpentier 1999; Mishra and Dubey 2005; Antal et al. 2009). Mercury increased the levels of photosynthetic pigments, viz., chlorophylls and carotenoids at a shorter exposure time but decreased the same at prolonged duration of exposure (Murthy et al. 1995). Hg^{2+} ions affected both light and dark reactions of photosynthesis and strongly inhibited the photosynthetic electron transport chain, Photosystem (PS) II being the most sensitive target. On the acceptor side, the inhibition was proposed by damage of the electron transfer from Q_A and Q_B and/or by increase of the fraction of closed (Q_A^-) reaction centers (RCs) (Kukarskikh et al. 2003). The donor side inhibition was manifested by prevention of the binding of chloride ions that act as a cofactor for the oxygen-evolving complex (OEC) and by selective removal of the 33-kDa extrinsic polypeptide associated with OEC (Bernier and Carpentier 1995). EPR spectroscopy showed that HgCl_2 released Mn^{2+} ions from the manganese cluster in the OEC and decreased the II_{slow} and $\text{II}_{\text{very fast}}$ signals of the intermediates Z_+/ D_+ , i.e., Tyr Z and Tyr D situated in the D1 and D2 proteins of PS II (Sersen et al. 1998). Mercury has been shown to react directly with plastocyanine, replacing copper (Kimimura and Kotoh 1972) and with the RC of PSI, oxidizing in the dark (Sersen et al. 1998). The high reactivity of mercury ions is proposed by formation of organometallic complexes with amino acids of photosynthetic proteins due to its strong affinity to C=O, C–N, C–S, and C–SH groups. This has been considered as possible mechanism (inhibitory effects) of Hg^{2+} on the photosynthetic apparatus (Bernier and Carpentier 1995). A fair number of similar studies but with much less details and results were reported on influence of mercury ions on cultures of photosynthetic bacteria. Long-term exposure of *Rhodobacter (Rba.) sphaeroides* (Giotta et al. 2006; Asztalos et al. 2010) or *Rhodospseudomonas capsulata*

(Jeffries and Butler 1975) to mercury resulted either in the prolongation of the lag phase or decrease in the growth rate. Half inhibitions values of 2–4 μM (*Rba. sphaeroides* wild type) and 20–30 μM (carotenoidless strain R-26.1) were reported. Proteomic analysis of intracellular membranes of *Rba. sphaeroides* R-26.1 cells grown in the presence of a high concentration (5 mM) of cobalt ions showed a change in the relative amount of proteins of the photosynthetic apparatus, with net downregulation of light-harvesting complexes and increased concentration of the nude RC, as well as upregulation of enzymes related to chemoorganotrophy (Italiano et al. 2011). These effects were considered to represent possible bacterial adaptation to retrieve energy for metabolic processes from sources alternative to less efficient photosynthesis. As very limited knowledge about the mercury attack on the photosynthetic apparatus of the bacteria is available, this work sets the aim to explore the direct effects of mercury ion on primary processes of bacterial photosynthesis and to reveal the molecular aspects of the mechanisms leading primarily to the observed changes (damages) in light-harvesting system and cyclic electron transport. The experiments are carried out with non-invasive (optical) methods on whole cells making possible to draw direct consequences to native systems. Beyond the significance of basic research, the present study may contribute to useful applications in conservation of the environment. The photosynthetic bacteria have been proved as highly promising candidates for bioremediation (Deng and Jia 2011) and seem to act as sponges for the heavy metals (Italiano et al. 2009) including mercury accumulated mainly in waterways as a consequence of anthropogenic activities. Finding out how the photosynthetic apparatus is affected by Hg^{2+} ions, potentially may be a viable way to combat the mercury pollution.

Materials and methods

Chemicals and bacterial strain

HgCl_2 , sodium citrate, and all chemicals (vitamins, growth factors, and buffers) required for bacterial cultivation were purchased from Sigma and used without any further purification. Cells of purple non-sulfur photosynthetic bacterium *Rba. sphaeroides* strain 2.4.1 were cultivated anaerobically in Siström (1962) medium in 1-l screw top flasks under continuous illumination of about 13 W m^{-2} provided by tungsten lamps (40 W). The cells were harvested at the late exponential phase of the growth and bubbled by nitrogen for 15 min before measurements. The mercury ion was added in form of HgCl_2 with equimolar amount of citrate to avoid the creation of poorly soluble mercury salts. The optical density of the samples was kept low ($\text{OD}(808\text{ nm}) < 0.1$) to keep the secondary effects (scattering, re-absorption of BChl fluorescence, secondary fluorescence, etc.) negligible compared to the primary signals (steady state absorption, light-induced absorption changes, prompt and delayed fluorescence (DL), etc.).

Absorption measurements

The steady state and room temperature absorption spectra of the cells were measured by Helios c spectrophotometer (Thermo Electron Corporation). After subtraction of the baseline due to light scattering, the narrow (750–950 nm) red part of the spectrum was decomposed into Lorentzian bands by method of least squares (Marquardt fit). The kinetics of absorption changes of the whole cells induced by Xe flash or by laser diode (Roithner LaserTechnik LD808-2-TO3, wavelength 808 nm and power 2 W) of rectangular shape (duration 1 ms) were detected by a home-constructed spectrophotometer (Maróti and Wraight 1988). The oxidized dimer (P^+) and the electrochromic shift of the carotenoids in the photosynthetic membrane were detected at 798 nm (Bina et al. 2009; Rivoyre et al. 2010) and 530 nm (with reference to 510 nm), respectively.

Fluorescence measurements

The induction of bacteriochlorophyll prompt fluorescence yield (Maróti 2008; Maróti and Wraight 2008; Kocsis et al. 2010) and the decay of the yield of DL (Filus et al. 2004; Asztalos and Maróti 2009) were measured by home-made kinetic bacteriochlorophyll fluorimeters. The prompt fluorescence of the bacteria (induction) was excited by pulsed laser diode (Roithner LaserTechnik LD808-2-TO3, wavelength 808 nm and power 2 W) and the DL by a Q-switched Nd-YAG laser (Quantel YG 781-10, wavelength 532 nm, energy 20 mJ, duration 5 ns). The fluorescence was detected through an IR cutoff filter (Schott RG-850) by a large area (diameter 10 mm) and high gain Si-avalanche photodiode (APD; model 394-70-72-581; Advanced Photonix, Inc., USA) for fluorescence induction and by a red-extended, cooled and electronically gated photomultiplier (Hamamatsu R-3310-03) in the mode of photon counting for DL. The intensities of the observed fluorescence were related to those of bacteriochlorophyll solution (prompt fluorescence) or heat-treated bacterium (80 C for short time) that had lost the DL but preserved the prompt fluorescence.

Results

One steady state and four kinetic assays are applied to follow the harmful effects of externally added mercury ions on the photosynthetic apparatus of intact cells of *Rba. sphaeroides*. The red part of the steady state absorption spectrum of the bacterium consists of three main bands centered at 800 and 850 nm reflecting the bacteriochlorophyll–protein complexes of the peripheral antenna and at 875 nm manifesting the bacteriochlorophylls of the core (antenna + RC) complex. The oscillatory strengths of these pigments are characterized by the area of the absorption bands. Upon mercury exposure of the cells, slight drop of the area of these bands can be observed on longer periods of time (Fig. 1) without significant shifts of the central wavelengths (the spectra are not shown). The marked difference between the band area of the untreated (control) and Hg^{2+} -treated cells under illumination (150 % after 8 h incubation, Fig. 1a) is due to the fact that the bacteria without mercury were growing while the cells with mercury were not (see for more information about the cell growth in Asztalos et al. 2010). The decrease of the oscillatory strengths is not uniform: the 800-nm band suffers larger drop than the other two bands. The continuous illumination of the bacteria during incubation with mercury ions accelerates the process of destruction but preserves the relation of changes observed in the dark.

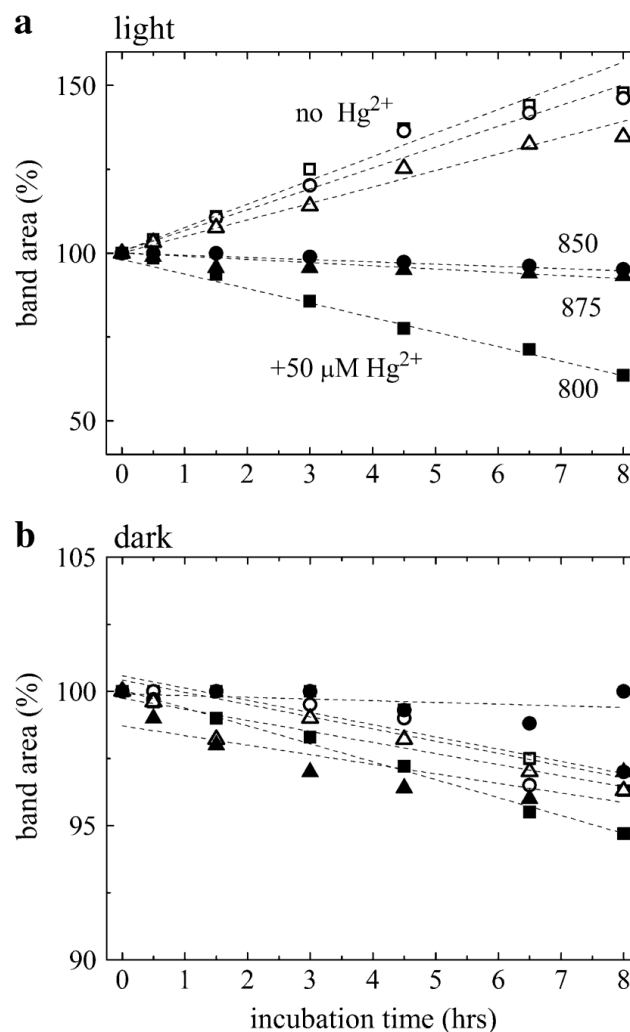


Fig. 1 Temporal changes of the area of steady state absorption bands of intact cells of photosynthetic bacterium *Rba. sphaeroides* 2.4.1 grown in the light (a) or kept in the dark (b) in the absence and in the presence of 50- μM HgCl_2 . The red parts of the absorption spectra were decomposed into three Lorentzian components of peaks at 800, 850, and 875 nm. Open square no Hg^{2+} B800, Filled square + Hg^{2+} B800, Open circle no Hg^{2+} B850, Filled circle + Hg^{2+} B850, Open triangle no Hg^{2+} B875, and Filled triangle + Hg^{2+} B875. Note the preferred loss of B800 in the light upon mercury treatment

The induction of the yield of bacteriochlorophyll fluorescence in the sub-millisecond time range reflects the photophysical process how the open RC receives electronic excitation and gets closed (Fig. 2). The details are included in three parameters: the initial (F_0) and final (F_{\max}) levels of fluorescence and the half rise time ($t_{1/2}$). (As the increase of the fluorescence yield follows complex kinetics, the introduction of the concept of half rise time does not need the peeling of the kinetics into (model-dependent) components.) Figure 3 shows the time-dependent variations of the fluorescence characteristics after the bacteria were treated by mercury ions and kept in light. The rises of F_0 and F_{\max} in the control sample are due to the growth of the culture. The general tendency of the mercury-treated sample is the continuous drop of F_{\max} while F_0 does not show significant changes during incubation. The variable fluorescence ($F_v = F_{\max} - F_0$) compared to the maximal fluorescence (F_v/F_{\max}) is generally considered as the measure of the photosynthetic activity of the bacterium. It performs large drop (from 0.75 to 0.50) within 3 h of treatment (Fig. 3c). The half rise time ($t_{1/2}$) does not change during the incubation significantly, but it is worth to mention its immediate decrease at the earliest Hg incubation time (Fig. 3d). By measuring the kinetics of the fluorescence induction of the bacteria, this effect can be used for early detection of mercury pollution of the culture (Asztalos et al. 2010).

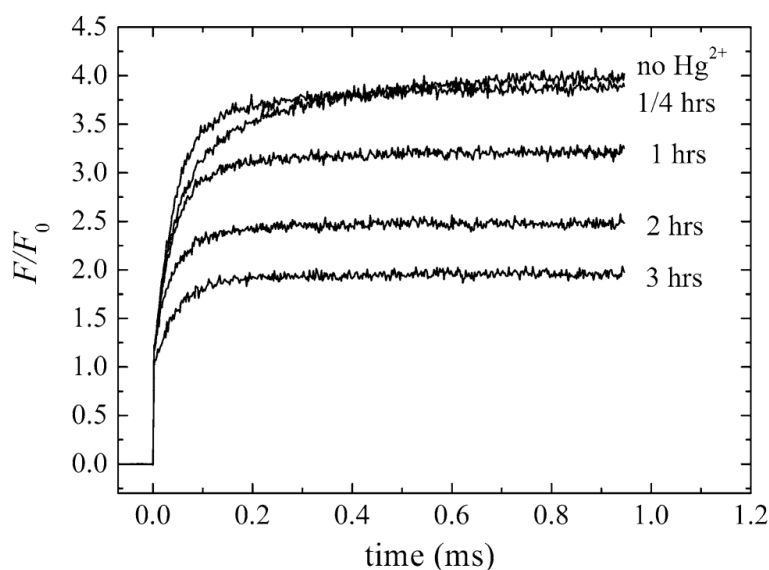


Fig. 2 Change of the bacteriochlorophyll fluorescence induction kinetics of whole cells kept in the light after selected time of incubation with of 26- μM mercury ions. The fluorescence was excited by rectangular shape of high power (2 W) laser diode at 808 nm. The actual intensity of fluorescence (F) was related to that of the initial fluorescence (F_0) resolved kinetically as the breaking point of the sudden initial rise of the fluorescence. The F_0 used for normalizing the vertical scale F/F_0 is measured in the absence of Hg^{2+} .

Complementary assay to the (quasi-steady state) fluorescence induction is the measurement of relevant absorption changes upon rectangular shape of laser diode excitation (Fig. 4.). The electrochromic response of the carotenoids detected as absorption change at 530 versus 510 nm wavelengths is an excellent indicator of the energization of the photosynthetic membrane after single (Fig. 4a) and several (Fig. 4b) turnovers of the RC not only for algae (Bailleul et al. 2010) but also for bacteria. The increase of the electrochromic change (Fig. 4b) is much slower than that of the fluorescence induction (Fig. 4d) measured under identical conditions of multiple turnovers although it includes a rapid but very small initial rise corresponding to closure of the RC. The changes of the electrochromic signal will include the degree of damage of intactness of the membrane and/or of the machinery of the cyclic electron transport upon mercury treatment (including the RC and the bc_1 complexes). The steady state level of the energization of the membrane is highly susceptible to the mercury concentration and can serve as a sensitive indicator of mercury pollution (Fig. 4c). As low as 5- μM Hg^{2+} causes significant damage of the membrane energy mainly by injured generation (via blocked electron transfer) of the energy. The decay time of the electrochromisms after single turnover flash is not modified by the mercury treatment significantly (Fig. 4a); therefore, the mechanism of increased dissipation may not play determining role in Hg^{2+} -induced loss of the membrane energy. To determine the changes of the rates of particular electron transfer reactions, absorption and fluorescence flash assays were applied. The oxidation of the dimer and the kinetics of subsequent re-reduction by cytochrome (cyt) c_2 were detected by flash-induced absorption change at 798 nm (Fig. 5a). The fast and slow components of the re-

reduction kinetics are attributed to electron donation from cyt *c*₂ close (attached) to the RC and distant from the RC, respectively. An additional very fast (10–20 μs) phase of cyt *c*₂ oxidation by P₊ was also reported and interpreted in terms of tight binding of the reduced cyt *c*₂ to the proximal site of the RC (Joliot et al. 1989). Based on experiments carried out with pre-oxidized cyt *c*₂ (not shown), we believe that the amplitude of the very fast component is small and may be neglected in the intact cells used here. Upon mercury treatment of the bacteria, the fast component of P₊ reduction converts to slow component gradually and finally the slow phase will disappear (Fig. 6). The decay of the P₊ amplitude at constant mercury concentration during incubation was fitted by a single exponential function and the rate constants showed clear linear dependence on the mercury concentration. This proves that the observed loss of P₊ is entirely due to Hg²⁺ incubation and a bimolecular rate constant of 34 h⁻¹ M⁻¹ can be derived (here the concentration of the externally added mercury should be taken into account). Use of weak (subsaturating) flashes, the P₊ to reduced cyt *c*₂ stoichiometric excess can be reduced and accordingly the slow component can be suppressed (Fig. 5b). The observation can be the consequence of changed stoichiometry of the species (there is enough pre-reduced cyt *c*₂ to react with the scarcer P₊) or can be related to the molecular organization of the photosynthetic apparatus like the RC–cyt *c*₂ supercomplex (Lavergne et al. 2008) or the heterogeneity (Crofts et al. 1998). If the sample is exposed to mercury ions, the fraction of the fast component of P₊ reduction will be smaller and independent on the flash intensity. The mercury decreases the P₊ to reduced cyt *c*₂ stoichiometric excess, and, perhaps, might have some effects on the structural arrangement of the proteins, as well.

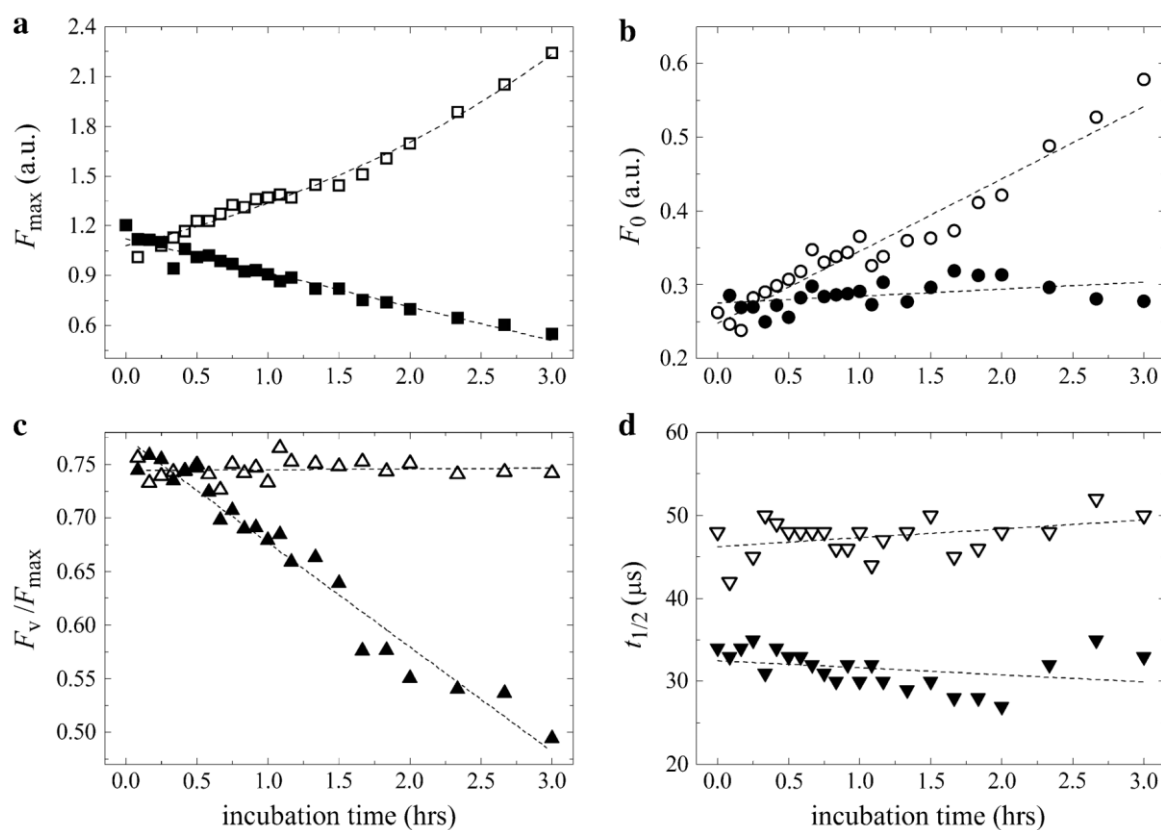


Fig. 3 Time-dependent changes of the fluorescence induction parameters of intact cells kept in the light in the absence (open symbols) and in the presence (closed symbols) of 26-μM Hg²⁺. Addition of mercury to the bacterial culture blocks the cell division immediately, decreases the maximum fluorescence level, F_{\max} (a), the variable fluorescence level ($F_v = F_{\max} - F_0$) compared to F_{\max} (c) and the half rise time, $t_{1/2}$ (d), and keeps the initial fluorescence level F_0 close to a constant value (b)

DL of the RC bacteriochlorophyll dimer is used to measure the free energy state and the lifetime of the P₊Q_A-charge separated state (Turzó et al. 2000). After addition of mercury to the culture, a sudden decrease of the amplitude can be observed without major changes in the kinetics (Fig. 7). The prompt effect of the Hg²⁺ incubation could not be kinetically resolved. On longer time scale (late effects of the mercury), both the amplitude and the rate constant of the decay are affected. While the amplitude decreases gradually, the rate constant of the decay increases. This tendency is well demonstrated by different representations of the area (intensity) of the DL ($\int DL$

dt vs. time of mercury treatment and $\int DL dt$ vs. Hg^{2+} concentration). In summary, the Hg^{2+} incubation makes the delayed emission smaller and faster within two kinetic steps, at least.

Discussion

The observed phenomena induced by the mercury ion will be discussed and interpreted in the frame of known primary processes in intact cells of the bacterium. The harvest and photochemical utilization of the light energy in photosynthetic bacterium *Rba. sphaeroides* are summarized in Fig. 8. The light is absorbed by one of the antenna pigments (A), which gets excited (A^*) and the electronic excitation energy is funneled to the open RC (Q_{AP}). Here, the bacteriochlorophyll dimer (P) becomes excited (P^*) that can lead to charge separation ($Q_A \cdot P^+$). The photochemistry is in competition with other deactivation processes of A^* including fluorescence and other loss processes. Part of the excitation energy transferred to the closed RC will be utilized for photochemistry by redirection to an open RC characterized by the interunit connectivity factor J. The charge separated state initiates a series of electron transfer reactions on the donor and acceptor sides of the RC. The oxidized dimer can be re-reduced either by a closely located (bound) or by a distant (unattached) reduced cyt c₂. The reduced primary quinone is oxidized by the secondary quinone. An extremely small fraction of the $Q_A \cdot P^+$ charge pair re-combines, re-populates the excited dimer and the antenna and delivers DL.

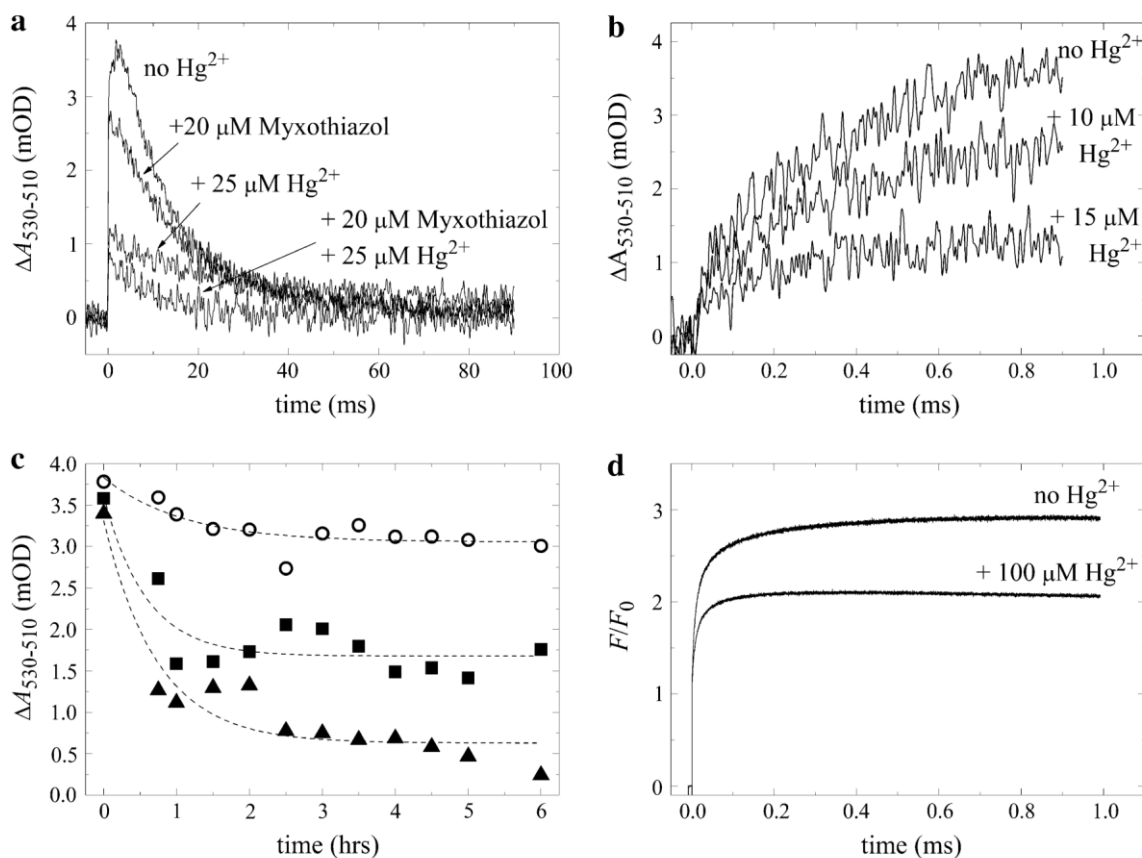


Fig. 4 Electrochromic response of the carotenoids measured by absorption change at 530 nm (vs. 510 nm) after single saturating flash excitation (a) and during continuous laser diode excitation (b) in the absence and in the presence of Hg^{2+} ions (1-h incubation time) and bc₁ inhibitor (myxothiazol). For comparison with (b), the fluorescence induction kinetics is also shown (d). Note the significant difference between the rates: the completion of the electrochromic signal needs multiple turnovers. The magnitude of the electrochromic rise (b) is a sensitive function of the Hg^{2+} concentration and the time of incubation (c)

The reduction of P^+ following a saturation flash can be decomposed into two phases. The fast phase in the 20–200- μ s range may arise from reduced cyt c₂ bound on a distal site of the RC or jump from other binding sites (e.g., bc₁ complex). The slow phase (200 μ s–20 ms) involves diffusion controlled shuttle of cyt c₂ between the RC and the bc₁ complexes. In isolated RC–cyt c systems, an additional and much faster ($\sim 1\mu$ s) component with 30–40 % of

the total was also observed that corresponded to RCs where the cyt c was bound at a proximal site (Mathis 1994). It was shown that the occupation of the proximal binding site and the rates of cyt-c-related electron transfer reactions were highly sensitive on the ionic strength of the solution (Overfield and Wraight 1986; Gerencsér et al. 1999). In intact cells of *Rba. sphaeroides*, the very fast component was not evident in our measurements, probably because of the non-negligible ionic strength around the intracytoplasmic membrane where the photosynthetic apparatus is located in the bacterium.

Effect of Hg²⁺ on light harvesting and on bacteriochlorophyll fluorescence

It was observed that after a prolonged (8 h) incubation of the cells with (50 μM) mercury, the 800-nm absorption band (*40 % in the light and *5 % in the dark) but not the 850-nm band (~5 %) showed preferential loss (Fig. 1). These two species are part of the peripheral antenna complex where they are bound in fixed ratio. The fact that only the 800-nm band is decreasing upon mercury treatment in the light indicates that the oligomeric ring of (8–9) ab heterodimers each associating three bacteriochlorophylls and one carotenoid should undergo structural and functional changes. The 800-nm bacteriochlorophyll–protein complex is targeted during prolonged mercury incubation. One of the most spectacular observations was the significant changes of the three (F_0 , F_{max} , and $t_{1/2}$) essential parameters of the fluorescence induction kinetics in the early phase of the mercury incubation (Figs. 2, 3) while the absorption of the bacterium did not show comparable modifications in this time range (Fig. 1). Although the characteristics of the fluorescence induction showed complex behavior on time and mercury concentration of the treatment, the general tendency of the drop of the maximum value (F_{max}) and the half rise time ($t_{1/2}$) could be recognized well. Based on the scheme of the light-harvesting processes (Fig. 8), the observed changes can be interpreted on a semiquantitative way by assuming direct effects of the mercury ion on the concentration of the photochemically active (open) RC and on the connectivity of the photosynthetic units (J). We argue that the Hg²⁺ ions getting inside the cell and close to the intracytoplasmic membrane decrease these quantities on a complex manner.

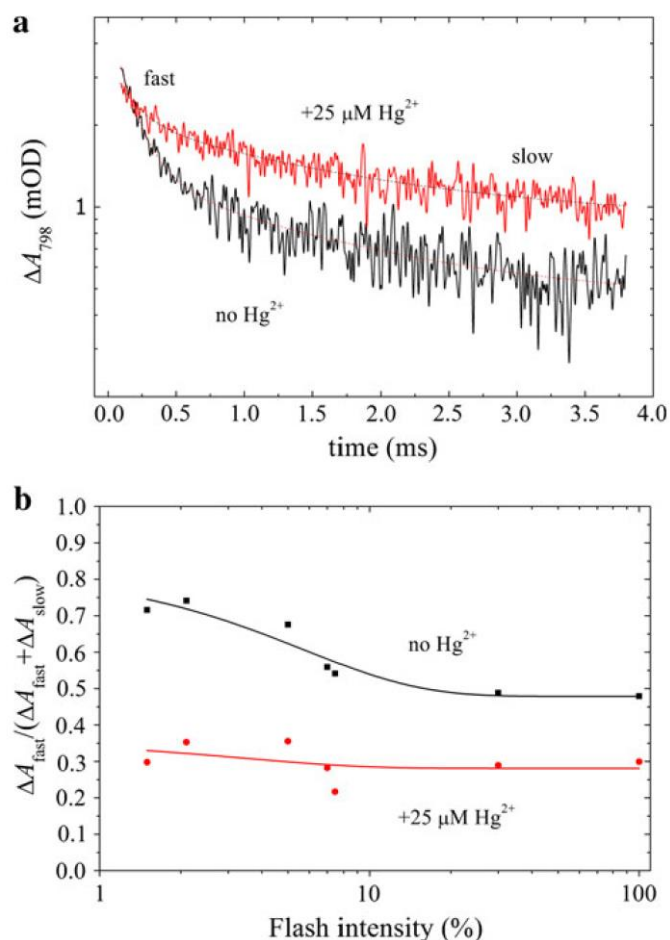


Fig. 5 Kinetics of flash-induced oxidation and re-reduction of the bacteriochlorophyll dimer (P) of intact cells of *Rba. sphaeroides* (a) and fraction of the fast phase of P⁺-re-reduction at attenuated Xe flash excitation intensities adjusted by

neutral density filters (b) in the absence and in the presence of Hg^{2+} (incubation time 0.5 h) monitored by absorption change at 798 nm. The traces are decomposed into fast and slow phases with amplitudes and rates of $DA_{\text{fast}} = 3.43 \text{ mOD}$ and $k_{\text{fast}} = (200\mu\text{s})^{-1}$ and $DA_{\text{slow}} = 1.10 \text{ mOD}$ and $k_{\text{slow}} = (4.66 \text{ ms})^{-1}$ for intact cells; and $DA_{\text{fast}} = 1.71 \text{ mOD}$ and $k_{\text{fast}} = (200\mu\text{s})^{-1}$ and $DA_{\text{slow}} = 1.84 \text{ mOD}$ and $k_{\text{slow}} = (5.68 \text{ ms})^{-1}$ for mercury-treated cells. In mercury-treated cells, the ratio of the amplitudes of the components becomes independent on the flash intensity

The yields of the fluorescence are

$$(F_0 \propto) \Phi_0 = \frac{k_f}{k_f + k_h + k_o \cdot [\text{RC}]} \quad (1)$$

in the initial state (when all RCs are open, $[\text{RC}]_o = [\text{RC}]$) and

$$(F_{\text{max}} \propto) \Phi_{\text{max}} = \frac{k_f}{k_f + k_h + k_c \cdot [\text{RC}]} \quad (2)$$

in the final state (when all RCs are closed, $[\text{RC}]_c = [\text{RC}]$). Here, k_f and k_h denote the rate constants of the photons in the antenna by fluorescence emission and by any other nonradiative (e.g., heat) loss processes, respectively. If the photochemical trapping is very efficient, then $k_o [\text{RC}] \ll k_f + k_h$. As the ratio of F_{max}/F_0 is about 4 (see Fig. 2), k_c & $k_o/4$, i.e., the rate of trapping of the photons by the closed RC becomes one-fourth of that of the open RC. The most remarkable effect of mercury on the fluorescence induction of intact cells is the significant drop of F_{max} , while F_0 remains practically constant (Fig. 3a, b). The initial fluorescence yield observed upon Hg^{2+} treatment is exposed to two opposite tendencies. From one side, the general fluorescence levels of the bacteria (including F_0) will drop due to the decreased absorption spectrum of the B800 band (Fig. 1), which is exclusively excited by the laser diode (808 nm) in our experiments. Although the B800 band is a LH2 component and contributes little to the observed fluorescence emission, its excitation is transferred to the emitting LH1 effectively. From the other side, the decrease of the concentration of the photoactive RCs due to the mercury treatment will increase F_0 (see Eq. 1). The two factors may have the same magnitude and this is why no significant changes of F_0 (at least compared to that of F_{max}) are observed upon mercury treatment. To explain the much larger change of F_{max} due to the mercury ions, it should be kept in mind that (from Eqs. 1, 2) any changes in the antenna (e.g., increase of k_h) would affect F_{max} more than F_0 . The observed effect on F_{max} , however, is still too large to be ascribed entirely to the same cause as that on F_0 . The decrease of F_{max} could be largely attributed to effects of the mercury on the RC. One possibility is the increase of the rate of trapping of the closed RC (k_c). Additional option is that the Hg^{2+} ion damages the acceptor side of the RC, slowing the re-oxidation of the reduced primary quinone (Fig. 8). Consequently, a fraction of the RCs will be trapped in the PQA^- state, which has less quenching than the closed RC with oxidized dimer (P^+QA^-). The decrease of the F_{max} level reflects the mercury-induced modification of the RC-LH1 complex. To explain the observed decrease of the half rise time of the fluorescence induction upon mercury treatment (Figs. 2, 3d, 4), the model of connected photosynthetic units will be applied (Lavergne and Trissl 1995)

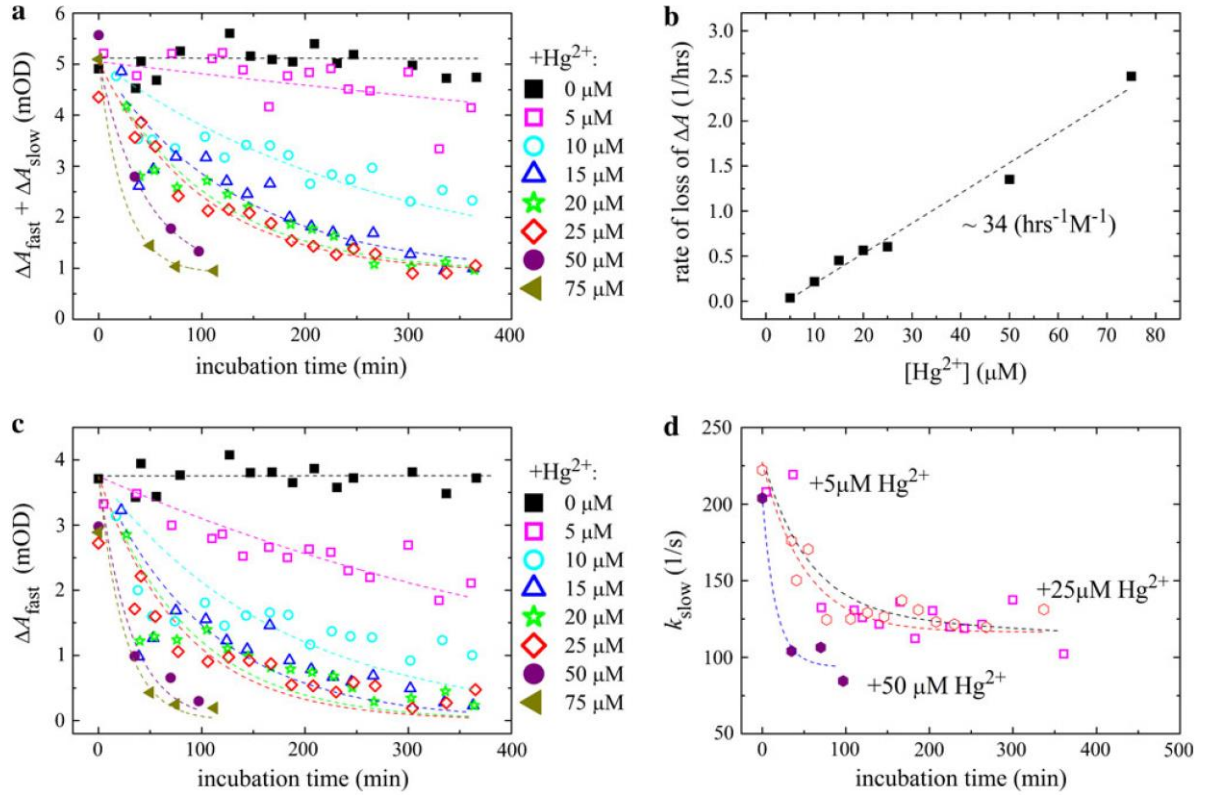


Fig. 6 Analysis of the re-reduction kinetics of flash-induced P₊ in mercury-treated cells as a function of Hg²⁺ concentration (5–75 μM) and incubation time (0–6 h). Temporal loss of the total amplitude at different mercury concentrations (a). Plot of the rate constants determined by monoexponential fit of curves on (a) against the mercury concentration (b). The loss of the amplitude of the fast component during incubation with different concentrations of mercury (c) is steeper than that of the total amplitude (see a). Decrease of the rate constant of the slow component during incubation at different mercury levels (d)

$$t_{1/2} = \frac{\ln(2+J)}{k_I} + \frac{J}{2+J}, \quad (3)$$

where k_I is the photochemical rate constant that depends on the light intensity (I), the absorption cross section of the antenna (σ) and the photochemical yield of the open RCs (Φ_p)

$$k_I = I \sigma \Phi_p = I \sigma \frac{k_o \cdot [\text{RC}]}{k_f + k_h + k_o \cdot [\text{RC}]} \quad (4)$$

The half rise time of the fluorescence induction characterizes all factors that contribute to the photochemical utilization of the excitation including the connectivity parameter among the photosynthetic units (J) which describes how much the closed RCs increase the actual cross section of the open units by re-direction of the excitation from the closed to the open units. The drop of $t_{1/2}$ upon mercury treatment of the bacteria can be attributed to changes of two essential parameters in Eqs. (3) and (4): the connectivity (J) and the concentration of photoactive RC. The J -dependence of $t_{1/2}$ is rigorously monotonous: by decrease of the connectivity, the half rise time will also decrease. For intact *Rba. sphaeroides* cells, $J \approx 1.0$ values are reported (Rivoyre et al. 2010; Maróti and Asztalos 2012) and Eq. (3) offers $t_{1/2} \approx 0.90/k_I$. If, however, the units become separated by the mercury treatment, then $J = 0$ and $t_{1/2} = 0.69/k_I$ that would involve about 25 % drop of the half rise time. As significantly smaller (*10 %) drop was observed in this work, it could be concluded that the mercury ions decreased but not disrupted the connection among the functional parts (photosynthetic units) of the light-harvesting system. More specifically, the connectivity in *Rba. sphaeroides* is mostly due to transfer within the RC–LH1 dimer (Rivoyre et

al. 2010). Any mercury-induced modifications that decrease the dimeric association of the RCs would lead to decrease of the connectivity.

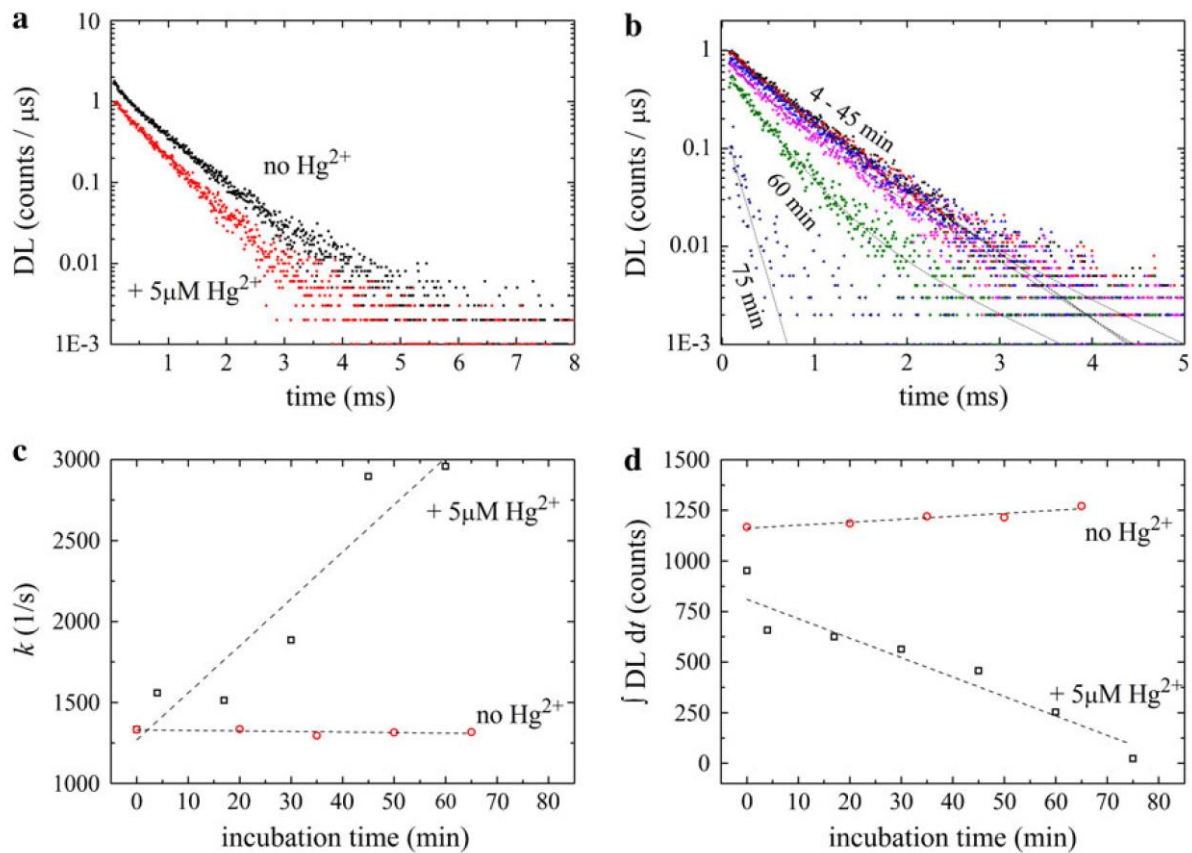


Fig. 7 Influence of mercury ions on the flash-induced DL of intact cells. Addition of 5- μ M Hg^{2+} causes immediate drop of the DL (a). Late effect of the mercury results in additional decrease of the amplitude accompanied by acceleration of the decay (b). The latter, in form of rate constant versus incubation time, is demonstrated in (c). As the two factors determine the area under the DL curve, their combined effect appears as sharp dependence of the intensity of DL on the time of incubation (d)

In native bacteria, the photochemical trapping is efficient ($k_0[\text{RC}] \gg k_f + k_h$) and therefore the photochemical rate constant (k_t) will depend on I and r only and not on $[\text{RC}]$ (Eq. 4). This means that the half rise time is independent on the concentration of the active RC (Eq. 3). In mercury-treated sample, however, the analysis becomes more complex. The different assays indicated in our experiments that the loss of photoactive RC became significant after exposure to high mercury concentration. If the damage of the photochemically active RC by Hg^{2+} treatment becomes so essential that $k_0[\text{RC}] \approx k_f + k_h$, then, according to Eq. (4), $t_{1/2}$ would be linearly proportional to $[\text{RC}]$, i.e., the half rise time of the fluorescence induction would drop parallel with the loss of the photoactive RCs induced by the mercury incubation.

Effect of Hg^{2+} on electron transport

Long enough exposure and high enough mercury concentration inhibit the cell division and lead to loss of the photosynthetic capacity of the bacterium. Our results shed some light how the mercury interacts with the photosynthetic apparatus and reveal the essential mechanisms that block the photosynthesis finally. The antenna system has proved to be less sensitive to the heavy-metal pollution than the primary redox system directly serving the primary charge pair in the RC. The mercury ion influences both the donor and the acceptor side redox reactions directly. The re-reduction kinetics of P^+ showed decrease both in amplitude and in rate after mercury treatment (Figs. 5, 6). That can be attributed to different levels of oxidation of the primary electron donor $\text{cyt } c_2^{2+}$ to P^+ . As the disappearance of the fast component is followed by deceleration of the slow component, it can be concluded that the bound $\text{cyt } c_2^{2+}$ is better exposed to Hg^{2+} oxidation than the $\text{cyt } c_2^{2+}$ molecules not attached to the RC. The mercury shifts the redox equilibrium of the mobile $\text{cyt } c_2^{2+}/\text{cyt } c_2^{3+}$ redox pair and the reduced fraction decreases.

Because the slow component of P_+ re-reduction is controlled by diffusion, the observed rate will decrease upon mercury pollution. The DL assay that measures the concentration of the charge pair $P_+Q_{A^-}$ and the free energy gap between P^* and $P_+Q_{A^-}$ (Maróti and Wraight 2008) can give information about the electron transfer reaction on the acceptor side if the kinetics of the re-reduction of P_+ is taken into account. Our results indicated that the kinetics of DL after mercury addition lost the amplitude and became faster (Fig. 7). Both the loss of active RC and increase of the Q_A/Q_{A^-} redox midpoint potential (increase of the free energy gap between P^* and $P_+Q_{A^-}$) due to Hg^{2+} can result in decrease of the amplitude of the DL signal. The acceleration of the decay is attributed to faster re-oxidation of Q_{A^-} by Q_B^- or directly by Hg^{2+} than that of the re-reduction of P_+ . The lifetime of Q_{A^-} is definitely decreased by mercury treatment. The assays based on quasi-steady state excitation probe changes of electron transfer steps outside the close vicinity of the RC and can measure the cyclic flow of the electrons. The electrochromic response of the carotenoids controlled by the energization of the photosynthetic membrane has proved to be a particularly sensitive assay of mercury pollution because the accumulation of the membrane energy became restricted after Hg^{2+} addition (Fig. 4b, c). Out of the two complexes which determine the kinetics of the carotenoid bandshift at 530 nm, the RC was found to be more susceptible to the mercury ion. The contribution of the two complexes to the electrochromic signal could be separated using known bc_1 inhibitors (Fig. 4a). In the presence of mercury, the signal size dropped dramatically due to the severe inhibition of the electron transfer through the RC. Although this effect alone diminished the function of the bc_1 complex, a non-negligible fraction of the smaller electrochrome signal remained sensitive to the specific bc_1 inhibitor. This can be considered as a qualitative indication for the higher stability of the bc_1 complex to the mercury pollution than that of the RC.

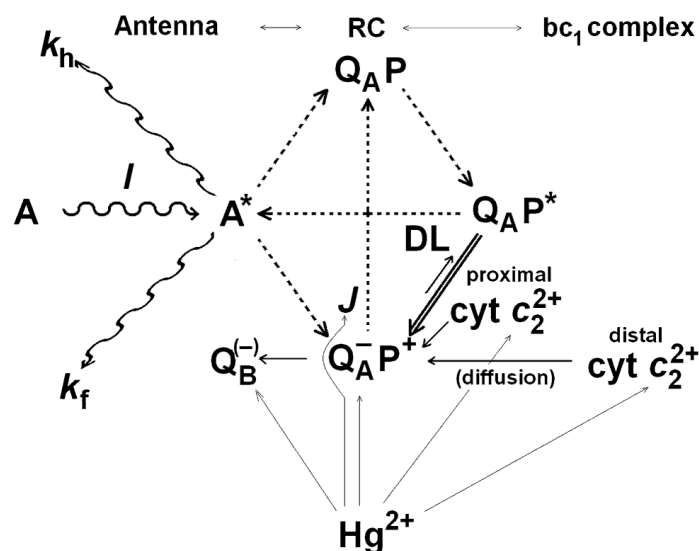


Fig. 8 Scheme of light funneling and primary electron transport processes in photosynthetic bacterium *Rba. sphaeroides* and possible targets of attack of the mercury ion (thin arrows). One of the antenna bacteriochlorophylls (A) is excited by light (I). A^* can be deactivated by fluorescence emission (rate constant k_f), by loss mechanisms (k_h), and by migration of the electron excitation (dashed arrows) to open (PQA) or closed ($P_+Q_{A^-}$) RCs. The excitons trapped by closed RC can be re-directed to (and utilized by) open RCs (J is the connectivity factor among the photosynthetic units). The excited dimer (P^*) initiates charge pair (double arrow) consumed by electron transfers (thick arrows) on the donor side by reduced $cyt\ c_2$ molecules either attached or unattached to the RC or on the acceptor side by oxidized (Q_B^-) or partly reduced (Q_B^-) secondary quinone. A very small fraction of the charge pair re-populates P^* and A^* that is deactivated in form of delayed light (DL)

Hg²⁺ uptake facilitated by metabolism in bacterium

The inhibition of photosynthesis by externally added mercury ions was much more pronounced in bacteria grown in the light than for those kept in the dark (Fig. 3c). This observation is in good accordance with the general view how the microorganisms cope with heavy-metal ion stress by combination of passive and active transport mechanisms. The Hg^{2+} ions are entrapped by the cellular surface via a non-specific, fast, and metabolic independent uptake (bioadsorption), but the cell wall creates an effective barrier hindering the passive penetration and the harmful effects on the photosynthetic apparatus in the intracytoplasmic membrane. Beside the less effective passive way, the mercury ions can be taken up in an active way by interaction with metabolic processes. Although

no specific mercury transport channels are developed in the bacterium, the Hg²⁺ ions can share transport mechanisms (channels) designed for other vital ions (Giotta et al. 2006; Italiano et al. 2009, 2011). In this “active” way, the bacterial metabolic cycles which are performed only by active and growing cell cultures can effectively increase the mercury bioaccumulation (Munoz and Guieysse 2006). Because the capacities and the rates of the transport mechanisms are very different, the harmful action of the mercury ions is expressed on a wide concentration and time scales including prompt and late effects.

Acknowledgments

We are indebted to Ms Diana Nyúli for absorption measurements in the early phase of this project and to the support of NKTH-OTKA (K-67850), TA ´ MOP 4.2.2/B, COST Action on “Molecular machineries for ion translocation across biomembranes” (CM0902) and MTA-CNR Bilateral agreement on “Bacterial photosynthesis: artificial photosystems and bioremediation”.

References

- Antal TK, Graevskaia EE, Matorin DN, Volgusheva AA, Osipov VA, Krendeleeva TE, Rubin AB (2009) Study of the effect of methylmercury and copper ions on primary photosynthesis processes in the green algae *Chlamydomonas moevusii* using the parameters of kinetic curves of the variable of chlorophyll fluorescence. *Biofizika* 54(4):681–687
- Asztalos E, Italiano F, Milano F, MarótiP, Trotta M (2010) Early detection of mercury contamination by fluorescence induction of photosynthetic bacteria. *Photochem Photobiol Sci* 9:1218–1223
- Asztalos E, MarótiP (2009) Export or recombination of charges in reaction centers in intact cells of photosynthetic bacteria *Biochim Biophys Acta* 1787:1444–1450.
- Bailleul B, Cardol P, Breyton C, Finazzi G (2010) Electrochromism: a useful probe to study algal photosynthesis. *Photosynth Res* 106(1–2):179–189
- Barregard L, Fabricius-Lagging E, Lundh T, Mo ´lne J, Wallin M, Olausson M, Modigh C, Sallsten G (2010) Cadmium, mercury, and lead in kidney cortex of living kidney donors: impact of different exposure sources. *Environ Res* 110:47–54
- Bernier M, Carpentier R (1995) The action of mercury on the binding of the extrinsic polypeptides associated with the water oxidizing complex of photosystem II. *FEBS Lett* 360:251–254
- Bina D, Litvin R, Va ´cha F (2009) Kinetics of in vivo bacteriochlorophyll fluorescence yield and the state of photosynthetic apparatus of purple bacteria. *Photosynth Res* 99:115–125
- Boca Raton Munoz R, Guieysse B (2006) Algal–bacterial processes for the treatment of hazardous contaminants: a review. *Water Res* 40:2799–2815
- Borsetti F, Martelli PL, Casadio R, Zannoni D (2009) Metals and metalloids in photosynthetic bacteria: interactions, resistance and putative homeostasis revealed by genome analysis. In: Hunter CN, Daldal F, Thurnauer MC, Beatty JT (eds) *The purple phototrophic bacteria*, Springer, Dordrecht, pp 655–689
- Boucher N, Carpentier R (1999) Hg²⁺, Cu²⁺, and Pb²⁺-induced changes in Photosystem II photochemical yield and energy storage in isolated thylakoid membranes: a study using simultaneous fluorescence and photoacoustic measurements. *Photosynth Res* 59:167–174
- Cain A, Vannella R, Woo LK (2008) Cyanobacteria as a biosorbent for mercuric ion. *Bioresour Technol* 99:6578–6586
- Clifton JC II (2007) Mercury exposure and public health. *Pediatr Clin North Am* 54(2):237–269
- Crofts A, Guergova-Kuras M, Hong S (1998) Chromatophore heterogeneity explains phenomena seen in *Rhodobacter sphaeroides* previously attributed to supercomplexes. *Photosynth Res* 55:357–362
- Deng X, Jia P (2011) Construction and characterization of a photosynthetic bacterium genetically engineered for Hg²⁺ uptake. *Bioresour Technol* 102:3083–3088
- Filus Z, Laczkó G, Wraight CA, MarótiP (2004) Delayed fluorescence from the photosynthetic reaction center measured by electronic gating of the photomultiplier. *Biopolymers* 74(1–2): 92–95
- Gerencsér L, Laczkó G, MarótiP (1999) Unbinding of oxidized cytochrome c from photosynthetic reaction center of *Rhodobacter sphaeroides* is the bottleneck of fast turnover. *Biochemistry* 38(51):16866–16875
- Giotta L, Agostiano A, Italiano F, Milano F, Trotta M (2006) Heavy metal ion influence on the photosynthetic growth of *Rhodobacter sphaeroides*. *Chemosphere* 62:1490–1499
- Gotsis-Skretas O (1991) Effects of mercury on cell population, chlorophyll a and rates of photosynthesis and excretion of *Dunaliella minuta* le arche. *Toxicol Environ Chem* 33:261–275
- Italiano F, Buccolieri A, Giotta L, Agostiano A, Valli L, Milano F, Trotta M (2009) Response of the carotenoidless mutant *Rhodobacter sphaeroides* growing cells to cobalt and nickel exposure. *Int Biodeterior Biodegradation* 63:948–957

- Italiano F, D'Amici GM, Rinalducci S, De Leo F, Zolla L, Gallerani R, Trotta M, Ceci LR (2011) The photosynthetic membrane proteome of *Rhodobacter sphaeroides* R-26.1 exposed to cobalt Res Microbiol 162(5):520–527
- Jeffries TW, Butler RG (1975) Growth inhibition of *Rhodospseudomonas capsulata* by methylmercury acetate. Appl Microbiol 30(1):156–158
- Joliot P, Vermeglio A, Joliot A (1989) Evidence for supercomplexes between reaction centers, cytochrome c2 and cytochrome bc1 complex in *Rhodobacter sphaeroides* whole cells. Biochim Biophys Acta 975(3):336–345
- Kamp-Nielsen L (1971) The effect of deleterious concentrations of mercury on the photosynthesis and growth of *Chlorella pyrenoidosa*. Physiol Plant 24(3):556–561
- Kimimura M, Kotoh S (1972) Studies on electron transport associated with photosystem II functional site of plastocyanin: inhibitory effects of HgCl₂ on electron transport and plastocyanin in chloroplasts. Biochim Biophys Acta 283:279–292
- Kocsis P, Asztalos E, Gingl Z, MarótiP (2010) Kinetic bacteriochlorophyll fluorometer. Photosynth Res 105:73–82
- Kukarskikh GL, Graevskaia EE, Krendeleva TE, Timofeedv KN, Rubin AB (2003) Effect of methylmercury on primary photosynthesis processes in green microalgae *Chlamydomonas reinhardtii*. Biofizika 48(5):853–859
- Lavergne J, Trissl H-W (1995) Theory of Fluorescence Induction in Photosystem II: Derivation of Analytical Expressions in a Model Including Exciton-Radical-Pair Equilibrium and Restricted Energy Transfer Between Photosynthetic Units. Biophys J 68:2474–2492
- Lavergne J, Vermeglio A, Joliot P (2008) Functional coupling between reaction centers and cytochrome bc1 complexes. In: Hunter CN, Daldal F, Thurnauer M, Beatty JT (eds) The purple photosynthetic bacteria. Springer, Dordrecht, pp 509–536
- Malik A (2004) Metal bioremediation through growing cells. Environ Int 30:261–278
- MarótiP (2008) Kinetics and yields of bacteriochlorophyll fluorescence: redox and conformation changes in reaction center of *Rhodobacter sphaeroides*. Eur Biophys J 37:1175–1184
- MarótiP, Asztalos E (2012) Calculation of connectivity of photosynthetic units in intact cells of *Rhodobacter sphaeroides*. In: Congming L (ed) Photosynthesis: research for food, fuel and future—15th international conference on photosynthesis, Symposium 02-01. Zhejiang University Press, Springer-Verlag GmbH, pp 27–31
- MarótiP, Wraight CA (1988) Flash-induced H⁺ binding by bacterial photosynthetic reaction centers: comparison of spectrometric and conductometric methods. Biochim Biophys Acta 934:314–328
- MarótiP, Wraight CA (2008) The redox midpoint potential of the primary quinone of reaction centers in chromatophores of *Rhodobacter sphaeroides* is pH independent. Eur Biophys J 37:1207–1217
- Mathis P (1994) Electron transfer between cytochrome c2 and the isolated reaction center of the purple bacterium *Rhodobacter sphaeroides*. Biochim Biophys Acta 1187:177–180
- Mishra S, Dubey RS (2005) Heavy metal toxicity induced alterations in photosynthetic metabolism in plants, Chapter 44. In: Pessaraki M (ed) Handbook of photosynthesis, 2nd edn. CRC Press,
- Murthy SDS, Mohanty N, Mohanty P (1995) Prolonged incubation of mercury alters energy transfer and chlorophyll (Chl) a protein complexes in *Synechococcus* 6301: changes in Chl a absorption and emission characteristics and loss of the F695 emission band Biometals 8:237–242
- Overfield RE, Wraight CA (1986) Photooxidation of mitochondrial cytochrome c by isolated bacterial reaction centers: evidence for tight-binding and diffusional pathways. Photosynth Res 9:167–179
- Panda S, Panda S (2009) Effect of mercury ion on the stability of the lipid-protein complex of isolated chloroplasts. Indian J Biochem Biophys 46:405–408
- Patra M, Bhowmik N, Bandopadhyay B, Sharma A (2004) Comparison of mercury, lead and arsenic with respect to genotoxic effects on plant systems and the development of genetic tolerance. Environ Exp Bot 52:199–223
- Patra M, Sharma A (2000) Mercury toxicity in plants. Bot Rev 66: 379–422
- Rivoyre M, Ginet N, Bouyer P, Lavergne J (2010) Excitation transfer connectivity in different purple bacteria: a theoretical and experimental study. Biochim Biophys Acta 1797:1780–1794
- Sersen F, Kralo 'va K, Bumbalova A (1998) Action of mercury on the photosynthetic apparatus of spinach chloroplasts. Photosynthetica 35:551–559
- Siström WR (1962) The kinetics of the synthesis of photopigments in *Rhodospseudomonas sphaeroides*. J Gen Microbiol 28:607–616
- Turzó K, Laczkó G, Filus Z, MarótiP (2000) Quinone-dependent delayed fluorescence from reaction center of photosynthetic bacteria. Biophys J 79(1):14–25.